https://doi.org/10.5194/amt-2020-305
Preprint. Discussion started: 2 September 2020

Atmospheric Measurement Techniques Discussions

Characterising water vapour concentration dependence of commercial cavity ring-down spectrometers for continuous onsite atmospheric water vapour isotope measurements in the tropics

Shujiro Komiya[1], Fumiyoshi Kondo[2], Heiko Moossen[1], Thomas Seifert[1], Uwe Schultz[1], Heike Geilmann[1], David Walter[1,3], and Jost V. Lavric[1]

[1]Max Planck Institute for Biogeochemistry, Jena, 07745, Germany
[2]Japan Coast Guard Academy, Kure, 737-8512, Japan
[3]Max Planck Institute for Chemistry, Mainz, 55128, Germany

* *Correspondence to:* Shujiro Komiya (skomiya@bgc-jena.mpg.de)

Abstract. The recent development and improvement of commercial laser-based spectrometers have expanded in situ continuous observations of water vapour (H_2O) stable isotope ratios (e.g., $\delta^{18}O$, $\delta^{2}H$, etc.) in a variety of sites worldwide. However, we still lack continuous observations in the Amazon, a region that significantly influences atmospheric and hydrological cycles on local to global scales. In order to achieve accurate on-site observations, commercial water isotope analysers require regular in situ calibration, including H_2O concentration dependence ([H_2O]-dependence) of isotopic accuracy. Past studies have assessed [H_2O]-dependence for air with H_2O concentrations up to 35,000 ppm, a value that is frequently surpassed in tropical rainforest settings like the central Amazon where we plan continuous observations. Here we investigated the performance of two commercial analysers (L1102i and L2130i models, Picarro, Inc., USA) for measuring $\delta^{18}O$ and $\delta^{2}H$ in atmospheric moisture at four different H_2O levels from 21,500 to 41,000 ppm. These H_2O levels were created by a custom-built calibration unit designed for regular in situ calibration. Measurements on the newer analyser model (L2130i) had better precision for $\delta^{18}O$ and $\delta^{2}H$ and demonstrated less influence of H_2O concentration on the measurement accuracy at each moisture level compared to the older L1102i. Based on our findings, we identified the most appropriate calibration strategy for [H_2O]-dependence, adapted to our calibration system. The best strategy required using two pairs of a two-point calibration with four different H_2O concentration levels. The smallest uncertainties in calibrating [H_2O]-dependence of isotopic accuracy of the two analysers were achieved using a linear-surface fitting method and a 28 h calibration interval, except for the $\delta^{18}O$ accuracy of the L1102i analyser for which the cubic fitting method gave best results. The uncertainties in [H_2O]-dependence calibration did not show any significant difference using calibration intervals from 28 h up to 196 h; this suggested that one [H_2O]-dependence calibration per week for the L2130i and L1102i analysers is sufficient.

1 Introduction

Ongoing climate change has affected various aspects of global and local climate, including the hydrological cycle (Intergovernmental Panel on Climate Change, 2014). Further and more detailed understanding on how climate change affects the atmospheric hydrological system is required. Water vapour isotope ratios (e.g., $\delta^{18}O$, $\delta^{2}H$, $\delta^{17}O$) have been used in meteorology and hydrology to disentangle the water vapour transport, mixing and phase changes such as evaporation and condensation that govern processes of the atmospheric hydrological cycle (Galewsky et al., 2016). Incorporating water vapour isotopic information into models has also improved simulations of hydrometeorological fields (Galewsky et al., 2016). The increase in field observation of water vapour isotope ratios therefore is expected to improve our process understanding and thereby models simulating the interactions between hydrometeorological cycles and global climate change.

https://doi.org/10.5194/amt-2020-305
Preprint. Discussion started: 2 September 2020

Atmospheric Measurement Techniques Discussions

Until around 10-15 years ago, *in-situ* water vapour isotope measurements were limited due to the laborious and error-prone sampling techniques using cryogenic traps, molecular sieves, vacuum flasks, etc. (Helliker and Noone, 2010). Recent development and improvement of laser-based spectrometers have made continuous water vapour isotope ratio measurements at a high temporal resolution possible. The number of onsite measurements of stable water vapour isotope ratios across the world has increased in the last decade (Wei et al., 2019). So far, field water isotopic measurements have been frequently conducted in North America, Europe, Africa, Asia, Oceania, Arctic and Antarctic regions (Wei et al., 2019), but not in South America including the Amazon basin region. Understanding the hydrological processes in the Amazon basin is crucial as it significantly influences the atmospheric convective circulation in the tropics and beyond (Coe et al., 2016; Galewsky et al., 2016b). Thus, in-situ measurements of water vapour isotope ratios in the Amazon region will improve our comprehension of the Amazonian hydro-climatological system and its interaction with global climate (Coe et al., 2016; Galewsky et al., 2016).

Recent field observations for water vapour isotopes have mainly utilized two commercial laser-based instruments: Picarro cavity ring-down spectroscopy (CRDS) and LGR off-axis integrated cavity output spectroscopy (OA-ICOS) analysers (Galewsky et al., 2016; Wei et al., 2019). The CRDS analysers have been used in most of the field sites that are registered in the Stable Water Vapor Isotopes Database (SWVID) website that archives onsite high-frequent water vapour isotope data (Wei et al., 2019). Globally, five CRDS models (i.e., L1102i, L1115i, L2120i, L2130i, L2140i sorted by oldest to newest) are in operation at various field sites and Aemisegger et al. (2012) confirmed that a newer model (L2130i) has better precision and accuracy compared to an older models(L1115i) due to the improved spectroscopic fitting algorithms.

Even with improved analysers, CRDS instruments still require regular calibration (e.g., 3-24 hour frequency) (Aemisegger et al., 2012; Delattre et al., 2015; Wei et al., 2019). The main calibration issue is that the measurement quality of water vapour isotopic ratios depends on water vapour (H_2O) concentration (hereinafter called "[H_2O]-dependence"; Schmidt et al., 2010, Tremoy et al., 2011, Aemisegger et al., 2012, Bailey et al., 2015, Delattre et al., 2015). The [H_2O]-dependence of Picarro analysers has been assessed over a H_2O concentration range spanning 200 to 35,000 ppm (Schmidt et al., 2010; Aemisegger et al., 2012; Steen-Larsen et al., 2014; Bailey et al., 2015; Delattre et al., 2015), and only rarely above 35,000 ppm (Tremoy et al. 2011). However, H_2O concentrations within the Amazon tropical rainforest canopy (e.g., the Amazon Tall Tower Observatory (ATTO) site; see Andreae et al 2015) normally exceed 35,000 ppm on a daily basis, with maximum concentrations reaching 44,000 ppm. Moreira et al. (1997) observed the diel variation pattern in H_2O concentration in the Amazon tropical rainforest was mostly similar to that in $\delta^{18}O$ and $\delta^{2}H$ of water vapour. The diel relationship between H_2O concentration and isotopes may lead to over- or under-estimation of isotopic values measured by CRDS analysers in the Amazon tropical rainforest. Thus, assuming in-situ water vapour isotope measurements by CRDS analysers in the Amazon tropical rainforest, the [H_2O]-dependence of CRDS analysers under high moisture conditions (> 35,000 ppm H_2O) needs to be assessed and corrected.

The primary aim of this study was to characterise two CRDS analysers (L1102i and L2130i) for measuring $\delta^{18}O$ and $\delta^{2}H$ of water vapour in high atmospheric moisture expected at the ATTO site, where we intend to conduct continuous in-situ observations. Over a two week periods, we examined the effects of H_2O concentration on isotopic measurement precision and accuracy for an older (L1102i) and a newer CRDS models (L2130i). We used a custom-made calibration system that regularly supplied standard water vapour samples at four different H_2O concentrations covering high moisture conditions (21,500 to 41,000 ppm) expected based on past measurement at the ATTO site. Standard water vapour samples were made from two standard waters, almost covering the previously reported isotopic ranges ($\delta^{18}O$ = -19.4 to -6.7 ‰ and $\delta^{2}H$ = -151 to -42 ‰) for water vapour samples in Manaus, located near the ATTO site, or in the Ducke Reserve near Manaus (Matsui et al., 1983; Moreira et al., 1997; IAEA/WMO, 2020). We also assessed which [H_2O]-dependence calibration strategy, based on the two-week operation, can reduce measurement uncertainty of the two CRDS models the most. According to the determined best calibration strategy, we discussed whether the CRDS analysers can sufficiently detect natural signals of stable water vapour isotopes, expected at the ATTO site.

https://doi.org/10.5194/amt-2020-305
Preprint. Discussion started: 2 September 2020

Atmospheric Measurement Techniques Discussions

2 Materials and Methods

2.1 Calibration system

We built a calibration system to routinely and automatically conduct onsite-calibration of CRDS analysers in the Amazon rainforest (Fig. 1). The main units of the calibration system are a syringe-pump, a vaporizer and a dry-air supply unit. The syringe-pump (Pump 11 Pico Plus Elite, Harvard Apparatus, Holliston, MA, USA) takes 3.3 mL standard water from a 2L reservoir bag (Cali-5-Bond^{TM}, Calibrated Instruments, Inc., Ardsley, New York, USA), and delivers the standard water into a vaporizer unit with a constant water flow of 1.9 µL min^{-1}. The vaporizer unit is comprised of a heater, vaporization chamber and buffer reservoir, which is enclosed in a copper pipe and heated at 140 $^{\circ}$C, covered by insulation material to reduce heat dissipation and help to reduce the memory effects between different water vapour isotopic measurements. Dried ambient air, recommended as a carrier gas for calibration by Aemisegger et al. (2012), was supplied into the heated vaporizer unit from a dry-air unit made up of a compressor, water separator, mist separators, membrane dryer (IDG60SAM4-F03C, SMC, Tokyo, Japan), precision regulator (IR1000, SMC, Tokyo, Japan) and flow regulator. The dry-air unit and mass flow controller 1 (MFC1) (1179B, MKS GmbH, Munich, Germany) provide the vaporizer unit with a steady flow of dried ambient air with a dew point temperature of -32 $^{\circ}$C or below, operated at 50 mL min^{-1} flow rate and 17.2-20.7 kPa flow pressure. The dry air entering the vaporizer is heated through the heater line, speeding up the evaporation of the infused standard water inside the vaporization chamber without fractionation. Furthermore, the heated carrier gas also reduces the memory effect on the measurements. The subsequent standard water vapour was well mixed inside a buffer reservoir, and then delivered through the multiposition valve (Model EMTMA-CE, VICI Corp., Houston, TX, USA), switching flow paths between the calibration and routine analysis mode of the two CRDS analysers: L1102i and L2130i. To minimise tubing memory effects on water vapour isotopic measurements, we connected the vaporizer unit and CRDS analysers with stainless steel tubing constantly held at 45 ^{o}C with heating tapes to avoid condensation inside the tubes (c.f., Schmidt et al., 2010, Tremoy et al., 2011). Before reaching the CRDS analysers, the transported standard water vapour was diluted with the dried ambient air via a dilution line and adjusted to an intended concentration level by regulating the dilution dry air flow rate using MFC2 (Fig. 1). The total flow rate of both the calibration and dilution lines exceeded the suction flow rates of the two CRDS analyzers. The excess air was exhausted through an overflow port.

2.2 Water vapour concentration dependence experiment

We conducted a continuous operation of the L1102i and L2130i analysers over a two-week period in June 2019 in an air-conditioned laboratory at Max Planck Institute for Biogeochemistry (MPI-BGC, Jena, Germany). The two CRDS analysers measured water vapour (H_2O) concentration, $\delta^{18}O$ and $\delta^{2}H$ of outside/room air samples from a profile gas-stream switching system (not shown in this article) or H_2O concentration, $\delta^{18}O$ and $\delta^{2}H$ of water vapour samples supplied from the calibration system (Fig. 1). Since H_2O concentration values measured by old CRDS models (e.g., L1102i) are biased due to the self-broadening effect of water vapour, H_2O concentration measuring by the L1102i were corrected following Winderlich et al., (2010) and Rella et al., (2013).

We also simulated regular automated calibration operation designed for field operations over the two-week period to regularly supply the two CRDS analysers with standard water vapour samples at four different concentration levels from 21,500 to 41,000 ppm. We prepared two different working standard waters (DI1 and DI2) made of deionized water to avoid clogging the heated tubes and chamber inside the vaporizer unit with salt compounds. Stable water isotope ratios ($\delta^{18}O$ and

https://doi.org/10.5194/amt-2020-305
Preprint. Discussion started: 2 September 2020

Atmospheric Measurement Techniques Discussions

δ^2H) of the DI1 and DI2 standards were analysed at the stable isotope laboratory (BGC-IsoLab) of the MPI-BGC using Isotope Ratio Mass Spectrometry (IRMS). For details on the IRMS technique, we refer readers to Gehre et al., (2004). The DI1 and DI2 standards were calibrated against VSMOW and SLAP via in-house standards: DI1-δ^{18}O = -25.07 ± 0.16‰, DI1-δ^2H = -144.66 ± 0.60‰, DI2-δ^{18}O = -3.69 ± 0.15‰, DI2-δ^2H = -34.30 ± 1.00‰ (also see the section S1 in the Supplement). The isotopic span of the DI1 and DI2 almost covers the previously reported range of δ^{18}O (-19.4 to -6.7 ‰) and δ^2H (-151 to -42 ‰) for water vapour samples in the Ducke Reserve near Manaus or in Manaus, located near the ATTO site (Matsui et al., 1983; Moreira et al., 1997; IAEA/WMO, 2020). For calibration, we alternated between the two standard waters. One calibration run required 75 minutes, of which the first 30 minutes were used for stabilizing the produced standard water vapours at the highest concentration level and delivering it to the CRDS analysers. Subsequently the calibration system created stepwise lower concentration levels of the standard water vapour every 15 minutes by regulating the dilution flow rate. One calibration run consisted of a 4-point concentration calibration at approximately 41,000 ppm, 36,000 ppm, 29,000 ppm, and 21,500 ppm. The actual measured mean and standard deviation of H_2O concentration at the respective four moisture level for all the calibration cycles during the two-week operation are shown in Table 1. The dilution flow rates for the different moisture levels were set to 9 sccm (41,000 ppm), 14 sccm (36,000 ppm), 21 sccm (29,000 ppm) and 28 sccm for 21,500 ppm. The set-point values were not changed during the 2-week test, thus simulating remote automatic onsite calibration runs. We used the last 7-minutes of data collected at each concentration level for the calibration assessment of the CRDS analysers. Immediately after a calibration cycle, the syringe-pump drained the remaining standard water inside the tube between the vaporization chamber and 3-way solenoid valve 1 (SV1) through the waste line and then washed the inner space between the vaporization chamber and the SV2 valve 3 times with the standard water scheduled for the next calibration cycle (Fig. 1). Subsequently, the rinsed vaporization chamber was fully dried with air from the dry-air unit for 2 to 4 hours. These rinsing and drying steps prevented any residual memory effect from the last calibration cycle on standard water vapour isotopic compositions during the next calibration run. We started the next calibration cycle seven hours after the start time of the last calibration cycle (i.e., the interval of the same working standard was 14 hours). Throughout the entire experimental period, the calibration system conducted automatically 24 calibration runs for each standard water, which used 160 mL each standard water in total.

We calculated isotopic deviations at each concentration level (hereinafter called "[H_2O]") for each calibration cycle to evaluate [H_2O]-dependence on isotopic measurement accuracy. The isotopic deviations at each [H_2O] were obtained from the difference between measured isotopic values at each [H_2O] during each calibration cycle and assigned reference values at 21,500 ppm on each calibration. Thus, the isotopic deviation values at 21,500 ppm are set to 0. We selected the 21,500 ppm level as the reference H_2O condition because Picarro guarantees high δ^{18}O and δ^2H precision of CRDS analysers between 17,000 – 23,000 ppm of H_2O, and to make the results comparable with a similar past study (Tremoy et al., 2011) that assigned 20,000 ppm as the reference level. The assignment of reference values for each calibration cycle enabled us to assess isotopic biases that were mainly due to [H_2O]-dependence but not other effects, e.g., drift effects on δ^{18}O and δ^2H accuracy between each calibration cycle.

2.3 Calibration for water vapour concentration dependence

We devised four strategies, referred to here as DI1, DI2, DI1-DI2*1Pair, DI1-2*2Pairs, to use the automated calibration system to determine and correct for [H_2O]-dependence, and used the two-week operation to assess which calibration strategy decreased the uncertainties in δ^{18}O and δ^2H measurements the most. Figure 2 summarises the overview of the four calibration strategies. D11 and D12 refer to the two standard waters, measured at the four different [H_2O]. For example, the DI1-2*2Pairs strategy uses two pairs of DI1 and DI2 calibration cycles (e.g., ID-**[3,4]**-**[7,8]** at 28 h interval) for obtaining calibration fittings of [H_2O]-dependence at intervals from 28 h to 196 h (Fig. 2). The DI1-2*2Pairs strategy utilized four two-

https://doi.org/10.5194/amt-2020-305
Preprint. Discussion started: 2 September 2020

Atmospheric Measurement Techniques Discussions

dimensional (2D) and a three-dimensional (3D) fitting methods (i.e., linear, quadratic, cubic, quartic, and linear-surface fitting methods) to obtain [H_2O]-dependence calibration fitting parameters.

As an example, Figure 3 illustrates five calibration fittings for [H_2O]-dependence of $\delta^{18}O$ accuracy for each CRDS analyser, acquired from two pairs of DI1 and DI2 calibration cycles (i.e., **3,4** and **7,8**) following the DI1-2*2Pairs strategy at a 28 h interval (also c.f., Fig. 2). The respective 2D fitting is acquired from a relationship between H_2O concentrations, measured at 4 different levels, and $\delta^{18}O$ deviation at each of the 4-point [H_2O] (the blue dots in Fig. 3). The linear-surface fitting also involves measuring the $\delta^{18}O$ value at each [H_2O] as an independent variable (Fig. 3). The procedure for calculating isotopic deviations at each [H_2O] was the same as described in section 2.2.

The quantitative evaluation of uncertainties in [H_2O]-dependence calibration was conducted by means of root mean square error (RMSE) between actual observed and predicted isotopic deviation values by obtained [H_2O]-dependence fittings. We calculated RMSE value for each of the [H_2O]-dependence 2D or 3D fittings as follows:

$$RMSE = \sqrt{\frac{1}{n}\sum_{i=1}^{n}\left(\delta_{(\mathrm{obs})} - \delta_{(pred)}\right)^2} \quad (1)$$

where $\delta_{(obs)}$ is the actual observed deviation value of $\delta^{18}O$ or $\delta^{2}H$ at each [H_2O] from measurement cycles, $\delta_{(pred)}$ is the predicted deviation value of $\delta^{18}O$ or $\delta^{2}H$ at each [H_2O], and n is the sample number. The measurement cycles represent calibration cycles that were not used for estimating [H_2O]-dependence, over an interval period between one or two calibration pairs. For example Figs. 2 and 3 show a 28 h interval using the DI1-2*2Pairs strategy with ID-**[3,4]-[7,8]**, where a DI1 and D2 calibration cycle (i.e., DI1: **5**, DI2: **6**) occurring in between are regarded as measurement cycles. The measured $\delta^{18}O$ deviation value at each [H_2O] during the measurement cycles (i.e., DI1: **5**, DI2: **6**) represents the value of $\delta_{(obs)}$ at each [H_2O] (the red and green dots in Fig. 3). The predicted isotopic deviation value (= $\delta_{(pred)}$) at each [H_2O] during the measurement cycles is calculated by each of the [H_2O]-dependence 2D or 3D fittings, applied to measured value of H_2O concentration at each [H_2O] or to measured values of both H_2O concentration and $\delta^{18}O$ at each [H_2O] during the measurement cycles (the open triangles in Fig. 3). The example of calculated $\delta^{18}O$ RMSE of each fitting method for each CRDS analyser is shown on each plot in Fig. 3.

We conducted $\delta^{18}O$ and $\delta^{2}H$ RMSE evaluation for all the [H_2O]-dependence fittings that were obtained from all the respective two pairs of DI1 and DI2 calibration cycles at each interval period (28 - 196 h) following the DI1-2*2Pairs strategy over the entire two-week period (c.f., Fig. 2). For instance, since the DI1-2*2Pairs strategy at 28 h interval formed 43 two pairs in total (i.e., **[1,2]-[5,6]**, **[2,3]-[6,7]**, **[3,4]-[7,8]** ~ **[42,43]-[46,47]**, **[43,44]-[47,48]**) (c.f., Fig. 2), we calculated $\delta^{18}O$ and $\delta^{2}H$ RMSE values for each of 43 [H_2O]-dependence linear, quadratic, cubic, quartic, or linear-surface fittings.

Compared with the DI1-2*2Pairs strategy, the DI1, DI2, and DI1-DI2*1Pair calibration strategies used a pair of only DI1 calibrations, a pair of only DI2 calibrations, and a pair of DI1 and DI2 calibrations, respectively, for acquiring [H_2O]-dependence fittings at intervals from 14 h to 196 h (DI1, DI2 calibration strategies) or from 21 h to 203 h (DI1-DI2*1Pair calibration strategy) (Fig. 2). The DI1 and DI2 calibration strategies utilized the four 2D fitting methods for obtaining [H_2O]-dependence calibration fittings, whereas the DI1-DI2*1Pair calibration strategy used the four 2D and one 3D fitting methods as with the DI1-2*2Pairs strategy. We also calculated RMSE value for each of the [H_2O]-dependence 2D or 3D fittings, obtained from each of all the pairs of only DI1 calibrations (DI1 calibration strategy), all the pairs of only DI2 calibrations (DI2 calibration strategy), or all the pairs of DI1 and DI2 calibrations (DI1-DI2*1Pair calibration strategy) at each interval period as well as the DI1-2*2Pairs strategy.

https://doi.org/10.5194/amt-2020-305
Preprint. Discussion started: 2 September 2020

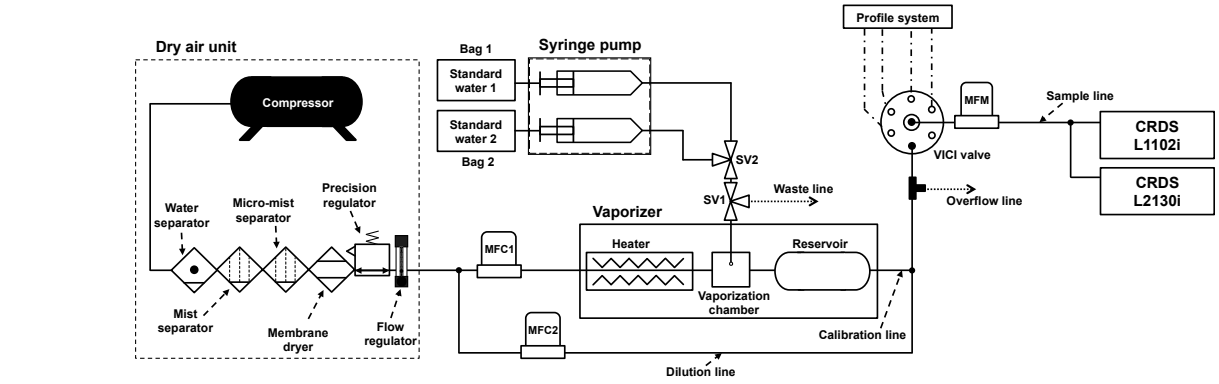

Figure 1 Schematic diagram of the calibration system. MFC, MFM and SV denote mass flow controller, mass flow meter, and 3-way solenoid valve, respectively. The profile system, prepared for in situ observation at the Amazon Tall Tower Observatory site (c.f., Andreae et al. 2015) in the Amazon tropical forest, is not described in this article. The diagram is not to scale.

Table 1 Standard deviations of $\delta^{18}O$ and $\delta^{2}H$ at each concentration level from all 24 calibration runs for the respective DI1 and DI2 standard waters. The standard deviations were calculated from all 24 data set of raw 7-min average values, obtained by L2130i and L1102i on each calibration run. The mean values of H_2O concentration at each concentration level were also calculated from all 24 data set of raw 7-min average values, obtained by L2130i and L1102i on each calibration run.

Precision (Standard deviation of all calibration runs at each H_2O concentration)

Picarro	Standard water					
	DI1 (n=24)			DI2 (n=24)		
	H_2O concentration (ppm)	$\delta^{18}O$ (‰)	$\delta^{2}H$ (‰)	H_2O concentration (ppm)	$\delta^{18}O$ (‰)	$\delta^{2}H$ (‰)
L2130i	21656.2 ± 243.6	0.09	0.45	21289.8 ± 220.0	0.08	0.55
	29144.1 ± 578.6	0.08	0.35	28473.0 ± 514.7	0.11	0.59
	36593.8 ± 676.2	0.13	0.68	35701.3 ± 565.7	0.12	0.68
	41803.0 ± 653.9	0.13	0.68	40744.4 ± 543.1	0.12	0.71
L1102i	20967.1 ± 253.5	0.14	1.01	20563.2 ± 244.9	0.11	0.99
	28957.3 ± 634.2	0.12	0.72	28244.0 ± 545.4	0.15	1.08
	37250.0 ± 756.5	0.18	0.90	36246.2 ± 690.1	0.20	1.06
	43387.8 ± 759.8	0.23	0.79	42172.1 ± 695.9	0.21	0.95

https://doi.org/10.5194/amt-2020-305
Preprint. Discussion started: 2 September 2020

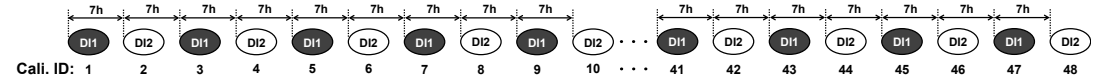

Calibration strategy	Interval (h)							
	14	21	28	35	42	~	196	203
DI1	**1 - 3** **3 - 5** **5 - 7** ~ **43 - 45** **45 - 47** (n = 23)	NA	**1 - 5** **3 - 7** **5 - 9** ~ **41 - 45** **43 - 47** (n = 22)	NA	**1 - 7** **3 - 9** **5 - 11** ~ **39 - 45** **41 - 47** (n = 21)	~	**1 - 29** **3 - 31** **5 - 33** ~ **17 - 45** **19 - 47** (n = 10)	NA
DI2	**2 - 4** **4 - 6** **6 - 8** ~ **44 - 46** **46 - 48** (n = 23)	NA	**2 - 6** **4 - 8** **6 - 10** ~ **42 - 46** **44 - 48** (n = 22)	NA	**2 - 8** **4 - 10** **6 - 12** ~ **40 - 46** **42 - 48** (n = 21)	~	**2 - 30** **4 - 32** **6 - 34** ~ **18 - 46** **20 - 48** (n = 10)	NA
DI1-DI2*1Pair	NA	**1 - 4** **2 - 5** **3 - 6** ~ **44 - 47** **45 - 48** (n = 45)	NA	**1 - 6** **2 - 7** **3 - 8** ~ **42 - 47** **43 - 48** (n = 43)	NA	~	NA	**1 - 30** **2 - 31** **3 - 32** ~ **18 - 47** **19 - 48** (n = 19)
DI1-DI2*2Pairs	NA	NA	**[1,2] - [5,6]** **[2,3] - [6,7]** **[3,4] - [7,8]** ~ **[42,43] - [46,47]** **[43,44] - [47,48]** (n = 43)	NA	**[1,2] - [7,8]** **[2,3] - [8,9]** **[3,4] - [9,10]** ~ **[40,41] - [46,47]** **[41,42] - [47,48]** (n = 41)	~	**[1,2] - [29,30]** **[2,3] - [30,31]** **[3,4] - [31,32]** ~ **[18,19] - [46,47]** **[19,20] - [47,48]** (n = 19)	NA

Figure 2 Overview of the four different [H_2O]-dependence calibration strategies (DI1, DI2, DI1-DI2*1Pair, DI1-2*2Pairs) for assessing [H_2O]-dependence uncertainties of the L2130i and L1102i analysers related to the length of the calibration interval. The top diagram shows a part of the total 48 calibration cycles, including both the DI1 and DI2 standard waters, with 7-hour interval and identity number (ID: **1** − **48**) as an example. The respective DI1 and DI2 strategies used a pair of only DI1 calibration cycles and a pair of only DI2 calibration cycles for obtaining calibration fittings of [H_2O]-dependence at intervals from 14 h to 196 h. The DI1-DI2*1Pair and DI1-2*2Pairs strategies used a pair of DI1 and DI2 calibration cycles, and two pairs of DI1 and DI2 calibration cycles, respectively, for obtaining calibration fittings of [H_2O]-dependence at intervals from 21 h to 203 h (DI1-DI2*1Pair strategy) or from 28 h to 196 h (DI1-DI2*2Pairs strategy). At each interval, the respective calibration strategy made all the pairs of each set calibration cycles (e.g., 43 two pairs at 28 h interval for the DI1-DI2*2Pairs strategy).

https://doi.org/10.5194/amt-2020-305
Preprint. Discussion started: 2 September 2020

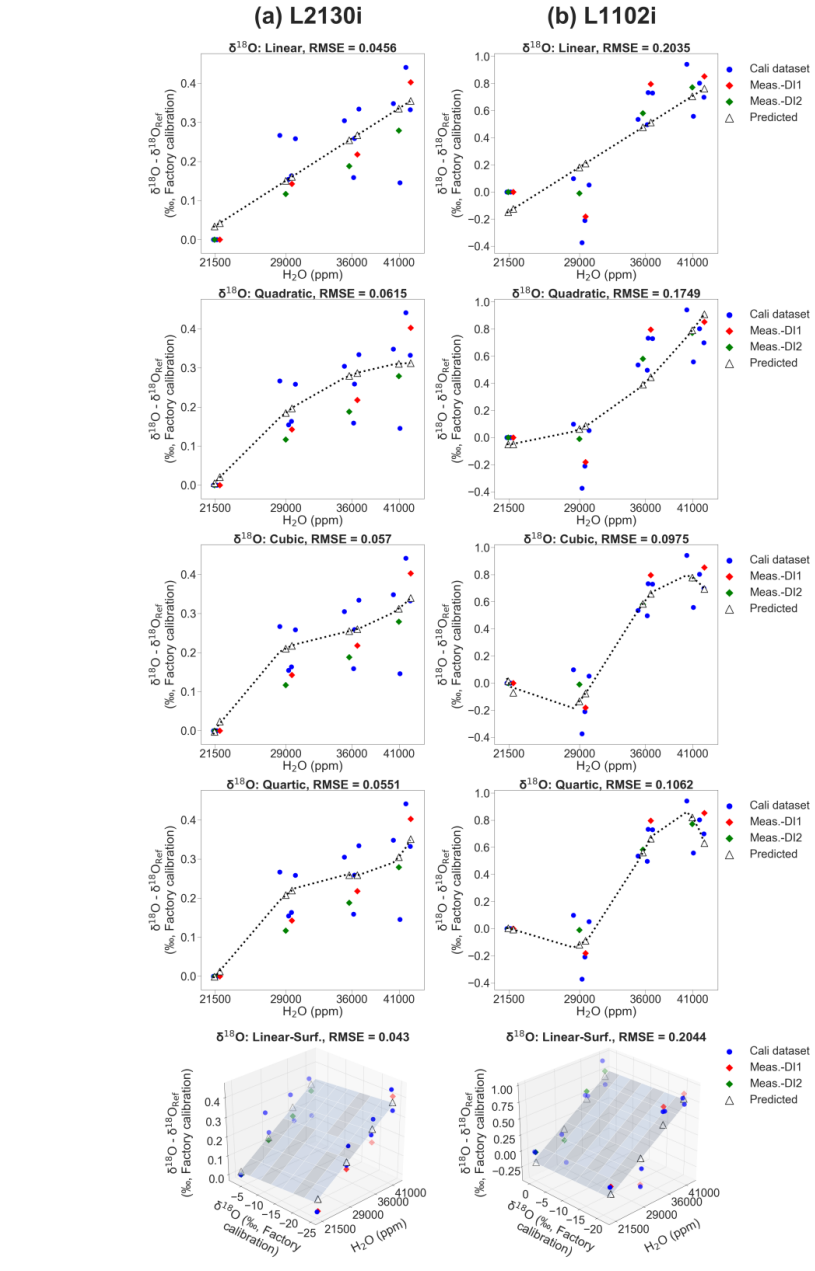

Figure 3 Example of calibrating [H_2O]-dependence of $\delta^{18}O$ accuracy for the respective (a) L2130i and (b) L1102i analysers by using four two-dimensional (2D) and a three-dimensional (3D) fitting methods (i.e., linear, quadratic, cubic, quartic, and linear-surface fitting methods) according to the DI1-2*2Pairs calibration strategy at 28 h interval with ID-**[3,4]** - **[7,8]** (c.f., Fig. 2). The blue dots on each plot represent data sets from two pairs of DI1 and DI2 calibration cycles (i.e., **[3,4]** and **[7,8]**) for obtaining each of the five calibration fittings. The respective 2D [H_2O]-dependence calibration fitting derives from a relationship between measured H_2O concentration and $\delta^{18}O$ deviation, equivalent to a difference between a measurement value of $\delta^{18}O$ at each of four concentration levels and that at 21,500 ppm level (=$\delta^{18}O_{Ref}$) on each calibration. The 3D [H_2O]-dependence calibration fitting also involves a measurement value of $\delta^{18}O$ value at each concentration level as an independent variable. The red and green diamonds denote the actual observed $\delta^{18}O$ deviations from unused DI1 (= ID-**5**) and DI2 (=ID-**6**)

https://doi.org/10.5194/amt-2020-305
Preprint. Discussion started: 2 September 2020

calibration cycles, respectively. The predicted $\delta^{18}O$ deviations, denoted as open triangles, on each plot were calculated from each [H_2O]-dependence calibration fitting, applied to measured H_2O concentrations (2D fitting methods) or to both measured H_2O concentration and $\delta^{18}O$ (3D fitting method) during the unused calibration cycles. The RMSE value on each plot was calculated from a difference between actual observed and predicted deviation values of $\delta^{18}O$.

3 Results and Discussions

3.1 Measurement precision over the two-week period

Figure 4 shows example times series of 7-min mean H_2O concentration, $\delta^{18}O$, and $\delta^{2}H$, calculated from raw L2130i measurement data for the highest and lowest H_2O concentrations (i.e., ~41,000 and ~21,500 ppm) over the entire DI1 standard water calibration runs for the two week period. The precision is defined as the standard deviation (σ) of all the raw 7-min average values over the 24 calibrations. The temporal changes in measured H_2O concentration at 21,500 ppm varied with H_2O-σ = 243.6 ppm (1.1%). over the whole period, whereas the highest moisture condition (= ~41,000 ppm) had larger variation of H_2O concentration (H_2O-σ: 653.9 ppm or ~1.5%; Fig. 4). The larger variability at 41,000 ppm likely derived from difficulty in establishing and delivering a stable high moisture stream from the calibration unit to L2130i, and possibly residual memory effects inside the tube line and L2130's measurement cell even with the well-heated condition (cell temperature = 80 °C) due to the extremely high moisture (> 40,000 ppm). One solution of the possible residual memory effects would be an increase in the tube-heater's temperature above 45 °C. Moreover, the less stable H_2O signal at the highest [H_2O] results in lower precisions of $\delta^{18}O$ (σ = 0.13‰) and $\delta^{2}H$ (σ = 0.68‰) compared with at the lowest [H_2O] ($\delta^{18}O$ -σ = 0.09‰ and $\delta^{2}H$ -σ = 0.45‰) (Fig. 4).

The larger variation in H_2O concentration at 41,000 ppm also implies instability of the calibration system, which possibly induces a decline in measurement precision of $\delta^{18}O$ and $\delta^{2}H$ values for the CRDS analysers at high humidity. Table 1 summarizes the precision of $\delta^{18}O$ and $\delta^{2}H$ for each [H_2O] on each standard water for the L2130i and L1102i analysers. The L2130i analyser has the highest precision of $\delta^{18}O$ measurement for the DI1 standard water at 29,000 ppm even though variability in H_2O concentration measurement was higher (H_2O-σ = 578.6 ppm at 29,000 ppm versus H_2O-σ = 243.6 at 21,000 ppm). Additionally, the L1102i analyser had higher $\delta^{18}O$ and $\delta^{2}H$ measurement precision at higher moisture conditions (≥ 29,000 ppm) than at the lowest moisture condition (= 21,500 ppm) for both the standard waters. The increase in measurement precision of L2130i and L1102i with [H_2O], despite larger [H_2O] variability, indicates that the instability of the calibration unit did not inherently exert a large influence on the measurement precision of the L2130i and L1102i analysers. Furthermore, the L1102i's $\delta^{18}O$ and $\delta^{2}H$ precision at 21,500 ppm ($\delta^{18}O$ -σ = 0.11-0.14‰ and $\delta^{2}H$ -σ = 0.99-1.01‰) were similar or better than those reported by Delattre et al. (2015) at 20,000 ppm for the L1102i ($\delta^{18}O$ and $\delta^{2}H$ precision of 0.08-0.19‰ and 1.5-2.0‰ respectively based on 40 calibration data over 35 days). This proves that the calibration system has a negligible effect on the isotopic measurement precision for L2130i and L1102i analysers.

At all H_2O concentration levels, and for both standard waters, the L2130i analyser had higher $\delta^{18}O$ (σ ≤ 0.11‰) and $\delta^{2}H$ (σ ≤ 0.59‰) precision under 30,000 ppm than over 30,000 ppm: $\delta^{18}O$ -σ ≥ 0.12‰ and $\delta^{2}H$ -σ ≥ 0.68‰ (Table 1). This indicates that the L2130i analyser can measure stable water isotopes more precisely for water vapour samples below 30,000 ppm. Compared to the L2130i analyser, the L1102i analyser had higher precision for only $\delta^{18}O$ below 30,000 ppm relative to over 30,000 ppm (Table 1). The different behaviour of both analysers described above would mainly be due to the old fitting algorithm used for the L1102i analyser (Aemisegger et al., 2012).

https://doi.org/10.5194/amt-2020-305
Preprint. Discussion started: 2 September 2020

Atmospheric Measurement Techniques Discussions

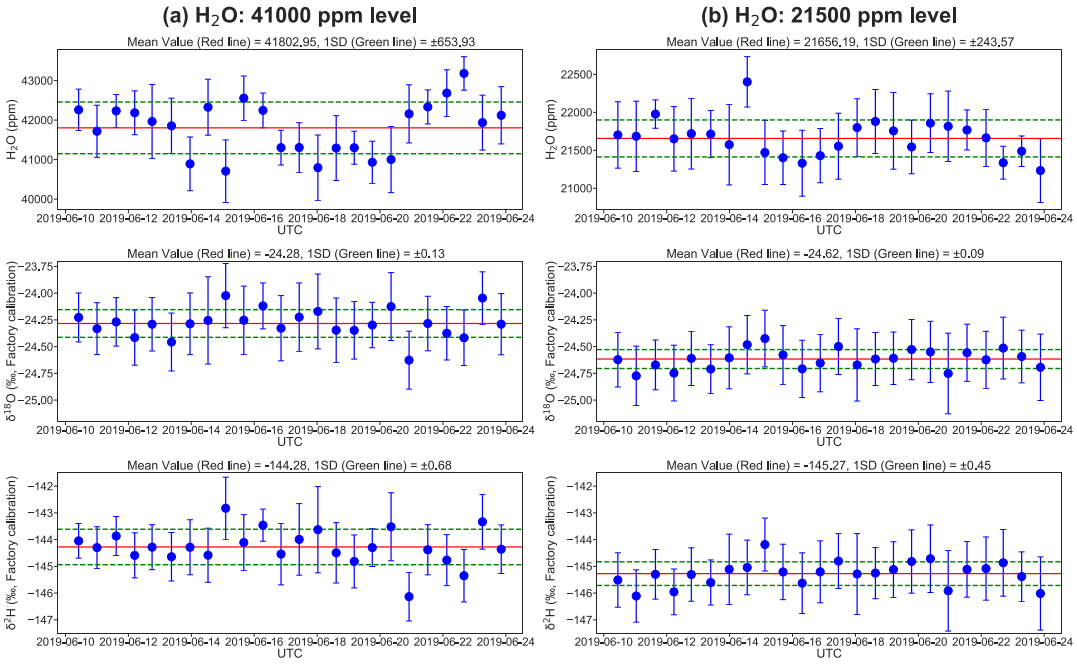

Figure 4 Two-week evolution of the L2130i's measurements for the DI1 standard water in H_2O concentration, $\delta^{18}O$, $\delta^{2}H$ at 41,000 ppm level (a), and at 21,500 ppm level (b). Each value is a 7-minute average of raw measurement data from the L2130i, and error bars are one standard deviation of 7-minutes. The red and green lines show the average and standard deviation through the 2-week measurement period.

3.2 Accuracy of isotope values for water vapour concentration dependence

For the L2130i analyser, the $\delta^{18}O$ deviation of both standard waters from reference values at 21,500 ppm gradually increased with H_2O concentration, reaching a maximum median value of 0.32‰ for DI1 and of 0.28 ‰ for DI2 (Fig. 5a). For $\delta^{18}O$, these differences were significant for both standard waters between 41,000 and 36,000 or 29,000 ppm (Fig. 5a, Welch's t-test, $p<0.01$), but differences between 36,000 and 29,000 ppm were not significant (Fig. 5a, Welch's t-test, $p>0.09$). As with $\delta^{18}O$, the values of $\delta^{2}H$ measured with the L2130i for both standard waters differed significantly between 41,000 ppm and the lower H_2O concentrations (Fig. 5b, Welch's t-test, $p<0.05$), without a significant difference between 29,000 ppm and 36,000 ppm (Fig. 5b, Welch's t-test, $p>0.86$). These results indicate accurate measurement of both $\delta^{18}O$ and $\delta^{2}H$ using the L2130i analyser require correction for [H_2O]-dependence under high moisture conditions (>36,000 ppm H_2O).

The differences in the deviation of each isotope from reference values at 21,500 ppm were similar for the two standard waters at all concentration levels except 41,000 ppm (Figs. 5a and 5b, Welch's t-test, $p>0.05$), where the L2130i indicated differences in $\delta^{2}H$ deviation for the two different standard waters (Figs. 5a and 5b, Welch's t-test, $p<0.05$). This finding indicates that the L2130i's $\delta^{2}H$ accuracy for high moisture like 41,000 ppm is dependent on the isotopic composition, thus more than one standard water needs to be used in the field.

The [H_2O]-dependence of $\delta^{18}O$ and $\delta^{2}H$ accuracy also gives rise to uncertainty in deuterium excess (hereinafter called d-excess, d-excess = $\delta^{2}H - 8\delta^{18}O$) values, estimated with the uncorrected $\delta^{18}O$ and $\delta^{2}H$ values (Figs. 5c and 5f). The d-excess deviation of the L2130i analyser significantly increased in a negative direction with concentration level on each standard water, and reached a maximum negative median value of -1.62 ‰ for DI1 and of -1.70 ‰ for DI2 (Fig. 5c). According to the calculation of d-excess, the decrease in d-excess with H_2O concentration mostly stemmed from the increase in the L2130i's

https://doi.org/10.5194/amt-2020-305
Preprint. Discussion started: 2 September 2020

Atmospheric Measurement Techniques Discussions

$\delta^{18}O$ values with H_2O concentration (Figs. 5a and 5c), which underlines the need for correcting for the [H_2O]-dependence, especially for $\delta^{18}O$ accuracy at high moisture levels using the L2130i analyser.

The L1102i also had strong [H_2O]-dependence for both isotopes, larger than that of the L2130i (Figs. 5a-b and 5d-e). The larger variations also led to large deviations in the d-excess values (Fig. 5f). In addition, both $\delta^{18}O$ and $\delta^{2}H$ accuracy for the L1102i depend on isotopic compositions ($\delta^{18}O$: 36,000 ppm, $\delta^{2}H$: all [H_2O]; Figs. 5d and 5e, Welch's t-test, $p<0.05$), different from the L2130i analyser. The above findings indicate that for the L1102i both $\delta^{2}H$ and $\delta^{18}O$ accuracy depend on H_2O concentration and the isotopic compositions, thus making the [H_2O]-dependence correction for both the $\delta^{2}H$ and $\delta^{18}O$ accuracy using different standard waters necessary.

The L1102i's result of $\delta^{18}O$ and $\delta^{2}H$ deviations were comparable with those reported by Tremoy et al. (2011) who checked [H_2O]-dependence on $\delta^{18}O$ and $\delta^{2}H$ accuracy for L1102i up to 39,000 ppm against the reference H_2O concentration at 20,000 ppm. However, Tremoy et al. (2011) observed negative $\delta^{18}O$ deviations at 39,000 ppm with a range between -2 and 0 ‰, different from this study. In addition, they confirmed a smaller increase in $\delta^{2}H$ deviations with H_2O concentration from 20,000 to 39,000 ppm than this study. The above differences in $\delta^{18}O$ and $\delta^{2}H$ deviations between Tremoy et al. (2011) and this study shows that [H_2O]-dependence of $\delta^{18}O$ and $\delta^{2}H$ accuracy must be evaluated for each individual analyser (Aemisegger et al., 2012; Bailey et al., 2015).

In summary, the measurement accuracy for in $\delta^{18}O$ and $\delta^{2}H$ is more dependent on H_2O concentration for the L1102i than the L2130i, mainly due to the older fitting algorithm for the initial version of the L1102i. In other words, the accuracy of [H_2O]-dependence of $\delta^{18}O$ and $\delta^{2}H$ for the L2130i has been improved due to the updated/corrected fitting algorithm (Aemisegger et al., 2012), but our results still remind us of the importance of correcting for the [H_2O]-dependence of $\delta^{18}O$ and $\delta^{2}H$ accuracy for the L2130i analyser, particularly for high moisture condition at 36,000 ppm and above.

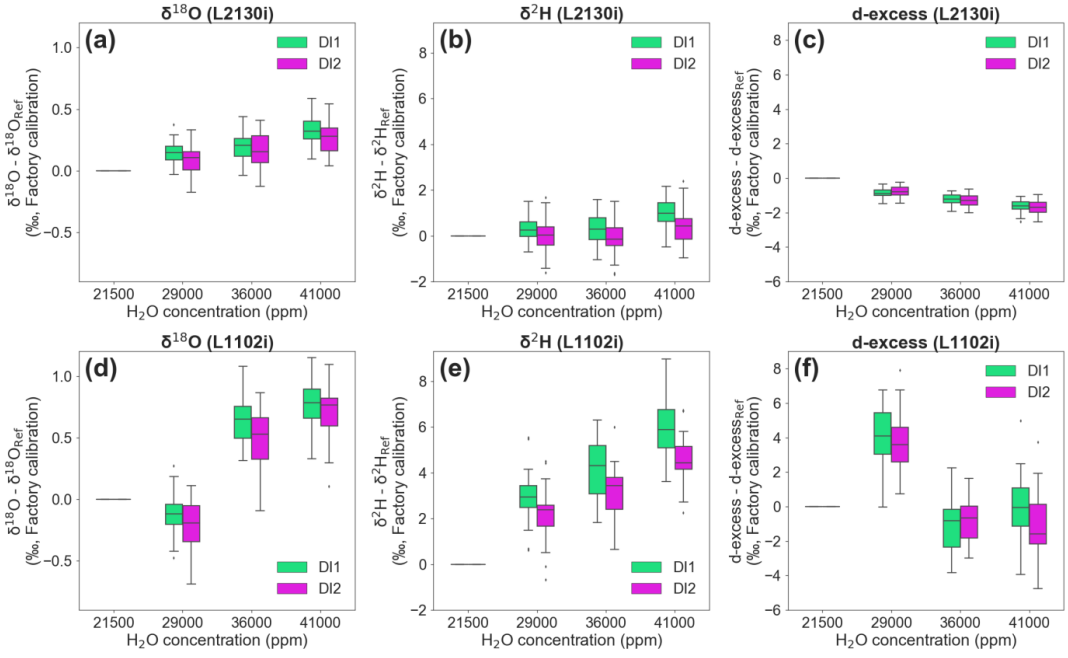

Figure 5 Deviations of stable isotopic compositions ($\delta^{18}O$, $\delta^{2}H$ and d-excess) for each standard water (DI1 and DI2) at three different H_2O concentrations compared to the 21,500 reference H_2O concentration. Boxplots of (a) $\delta^{18}O$, (b) $\delta^{2}H$, and (c) d-excess deviations, measured by L2130i. Boxplots of (d) $\delta^{18}O$, (e) $\delta^{2}H$, and (f) d-excess deviations, measured by L1102i. The $\delta^{18}O$, $\delta^{2}H$ and d-excess values at 21,500 ppm are assigned a value of 0, and [H_2O]-dependence for each isotope can be observed as the deviation between the value at each [H_2O] from the value measured at 21,500 ppm.

https://doi.org/10.5194/amt-2020-305
Preprint. Discussion started: 2 September 2020

Atmospheric Measurement Techniques Discussions

3.3 Strategy for calibration of isotope values for water vapour concentration dependence

The four calibration strategies for correcting isotope values using measured H_2O concentrations are compared in Figure 6. Across methods, the L2130i analyser usually displays lower median RMSE values compared to the L1102i analyser (Fig. 6). This tendency is also found in δ^2H RMSE results on each calibration strategy (see Fig. S1 in the Supplement). The lower RMSE values of the L2130i analyser indicate that a [H_2O]-dependence calibration increases accuracy of water vapour isotope measurements more for the L2130i analyser than the L1102i analyser.

The lowest median RMSE for the L1102i analyser is the cubic fitting method (Fig. 6). Among all the calibration strategies of the L1102i analyser, the DI1-2*2Pairs calibration strategy with the cubic fitting method usually shows the minimum median RMSE value for $\delta^{18}O$ accuracy (Fig. 6). For δ^2H accuracy of the L1102i analyser, the DI1-2*2Pairs calibration strategy also usually displays lower median RMSE values relative to the other strategies. These results indicate that this calibration strategy is most appropriate for correcting [H_2O]-dependence and improving the accuracy of isotope measurements with the L1102i analyser.

Compared with the L1102i analyser, the DI1-2*2Pairs calibration strategy of the L2130i analyser does not show clearly reduced isotopic RMSE values relative to the other calibration strategies, but still displays low RMSE values with a small distribution from each fitting method at each interval (Figs. 6 and S1). This indicates that the DI1-2*2Pairs strategy can be utilized for correcting [H_2O]-dependence of the L2130i analyser as well as the L1102i analyser. Since the calibration system uses the same tube line between the vaporizer and the branch point before the inlet port of each CRDS analysers (Fig. 1), we decided to utilize the DI1-2*2Pairs strategy for the L2130i analyser in the same way as the L1102i analyser.

The respective CRDS analyser with the DI1-2*2Pairs strategy shows a similar range of RMSE among the five curve-fitting methods (Figs. 6 and S1). The results do not clearly indicate which fitting method most frequently obtains the lowest RMSE values for each [H_2O]-dependence calibration interval. Hence, we report differences among fitting methods in detail only for the DI1-2*2Pairs strategy (Fig. 7). The linear-surface fitting method most frequently gives the lowest isotopic RMSE values, except $\delta^{18}O$ accuracy of the L1102i analyser (i.e., cubic fitting method), at 28 h interval (Fig. 7). This indicates that the linear-surface fitting method at 28 h interval reduces uncertainties in correcting [H_2O]-dependence on isotopic accuracy most effectively, except for $\delta^{18}O$ accuracy of the L1102i analyser. Compared with 28 h interval, the 2D fitting methods are the most appropriate for calibrating [H_2O]-dependence on isotopic accuracy over long intervals, excluding δ^2H accuracy of the L1102i analyser (Fig. 7). The difference in fitting methods between 28 h and longer intervals suggests that the 28 h interval strategy can correct for both [H_2O]- and isotope-dependent errors by using the 3D fitting method, whereas the long interval strategies can correct for only [H_2O]-dependent errors with the 2D fitting methods.

Each CRDS analyser using the DI1-2*2Pairs strategy shows the lowest median RMSE values of isotopic accuracy at the shortest interval (= 28 h), which only slightly increases with interval over 8 days (Fig. 6). This suggests that more frequent [H_2O]-dependence calibrations in high moisture environments can improve $\delta^{18}O$ and δ^2H accuracy unless the frequent calibrations use up standard water on site. However, at remote field sites where logistics is restricted, the above findings for the interval period also support that one [H_2O]-dependence calibration per week is enough to maintain good isotopic measurement of the CRDS analysers for an in-situ continuous observation remotely. Additionally, the RMSE distribution of isotopic accuracy gradually gets smaller with interval over 8 days (Fig. 6). The smaller RMSE distributions at long intervals result from larger sample numbers for calculating RMSE values at long intervals, whereas the larger RMSE distributions at short intervals is attributed to smaller sample numbers for calculating RMSE (28 h: n=43, 196 h: n=19; c.f., Fig. 2).

Although our results suggest one [H_2O]-dependence calibration per week is enough, to be on the safe side, we decided to conduct the [H_2O]-dependence calibration at 28 h or less interval with the DI1-2*2Pairs strategy. Figure 8 presents the corrected isotope deviations by the best fitting methods (L2130i and L1102i-δ^2H: linear-surface fitting, L1102i-$\delta^{18}O$: cubic

https://doi.org/10.5194/amt-2020-305
Preprint. Discussion started: 2 September 2020

Atmospheric Measurement Techniques Discussions

fitting) at 28 h interval. The isotope deviations of each CRDS analysers do not substantially vary with H_2O concentration. This indicates the calibrations successfully corrected [H_2O]-dependence of isotope accuracy for each analysers. Based on Moreira et al. (1997), water vapour isotope values in Amazon rainforest is expected to change diurnally by up to 2‰ ($\delta^{18}O$) or 4-8‰ ($\delta^{2}H$) with H_2O concentration. The diel isotope variations are higher than the corrected deviation values of each CRDS analyser (Fig. 8). This supports that both the CRDS analysers will detect diel or probably seasonal/interannual variations in water vapour isotopes in Amazon rainforest.

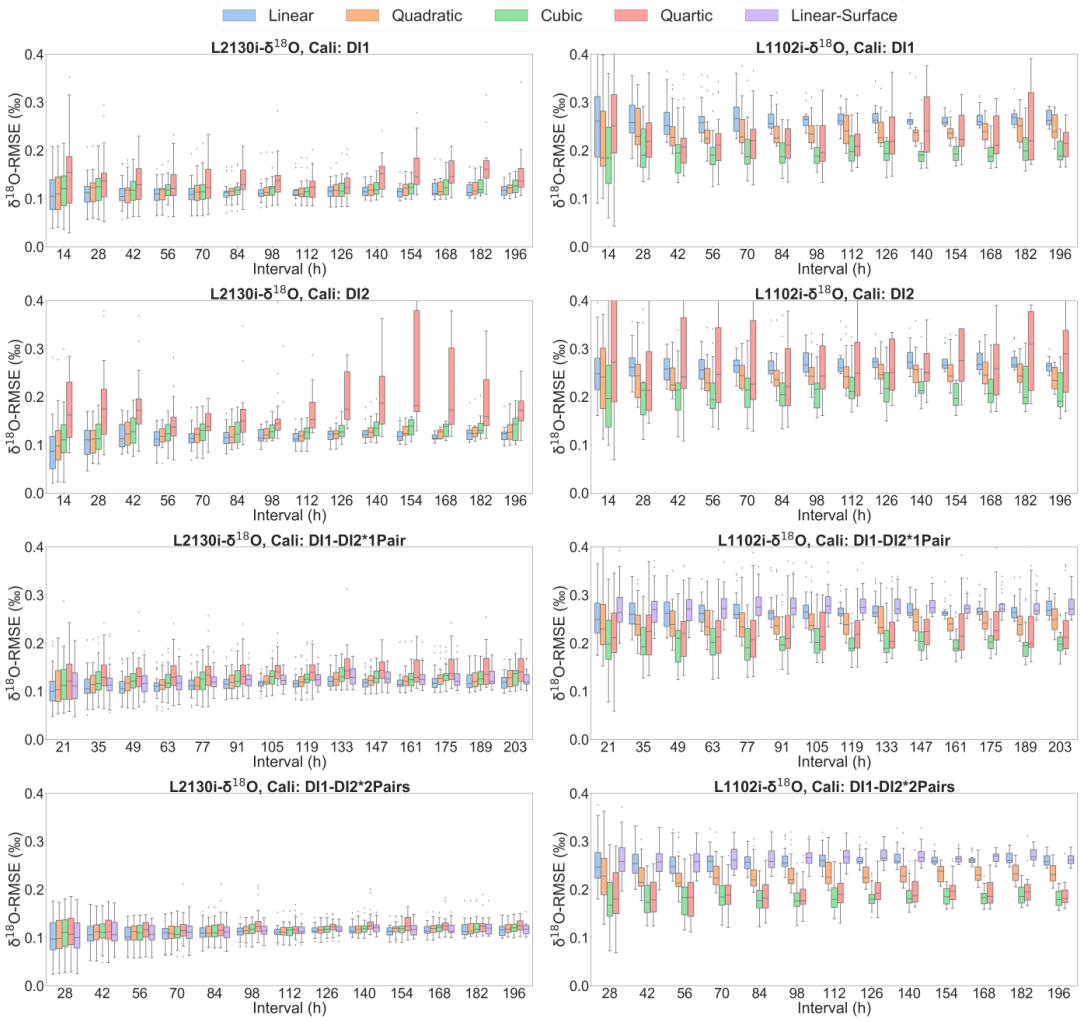

Figure 6 Boxplots of root mean square error (RMSE) of $\delta^{18}O$, derived from calibrating [H_2O]-dependence of $\delta^{18}O$ measurements by each of five fitting methods (i.e., linear, quadratic, cubic, quartic, linear surface fitting methods) for each of four calibration strategies: DI1, DI2, DI1-DI2*1Pair, DI1-2*2Pairs. The left-hand figures present boxplots of RMSE of $\delta^{18}O$ measurements by the L2130i, depending on interval length (i.e., the time period used for calibrating [H_2O]-dependence). The right-hand figures display boxplots of RMSE of $\delta^{18}O$ measurements by the L1102i, depending on interval length. The procedure for assessing [H_2O]-dependence uncertainties (= RMSE) is described in section 2.3.

https://doi.org/10.5194/amt-2020-305
Preprint. Discussion started: 2 September 2020

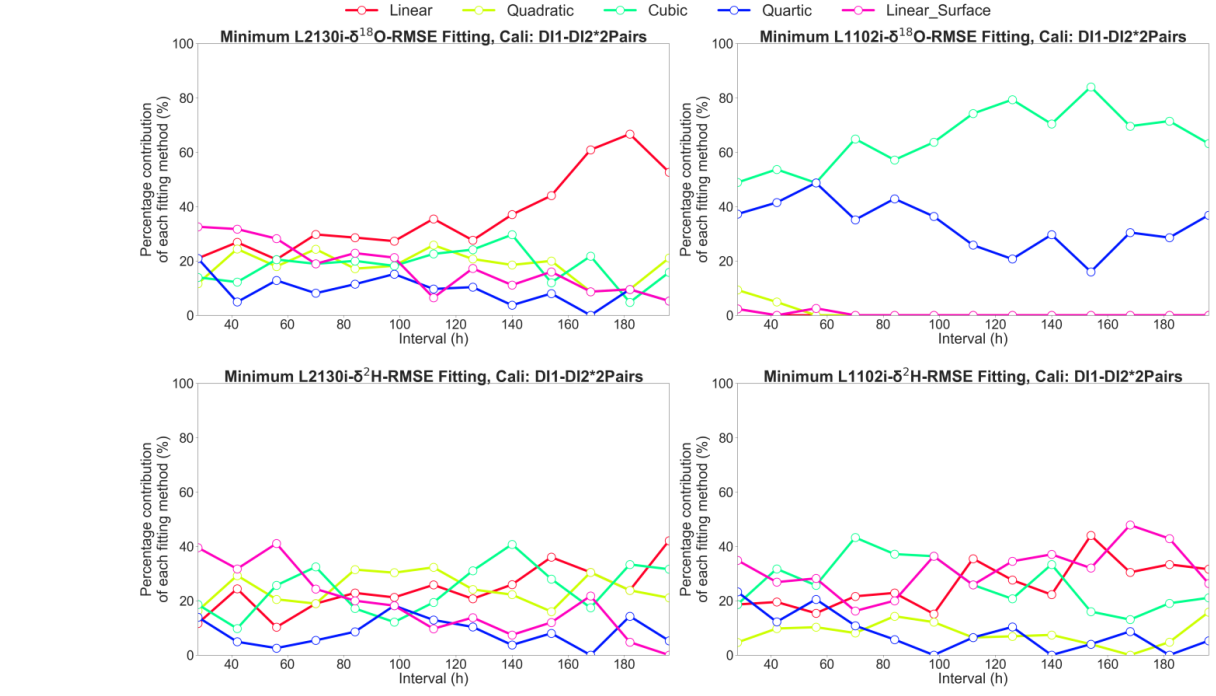

Figure 7 Percentage contribution of the respective five [H_2O]-dependence fittings (i.e., linear, quadratic, cubic, quartic, linear surface fitting methods) to the total calibration pairs, which only obtained minimum RMSE values of $\delta^{18}O$ and $\delta^{2}H$, at each interval for the DI1-2*2Pairs calibration strategy. The left-hand and right-hand figures present results of the L2130i, and of the L1102i, respectively. The top and bottom figures present results of $\delta^{18}O$ RMSE, and of $\delta^{2}H$ RMSE, respectively.

https://doi.org/10.5194/amt-2020-305
Preprint. Discussion started: 2 September 2020

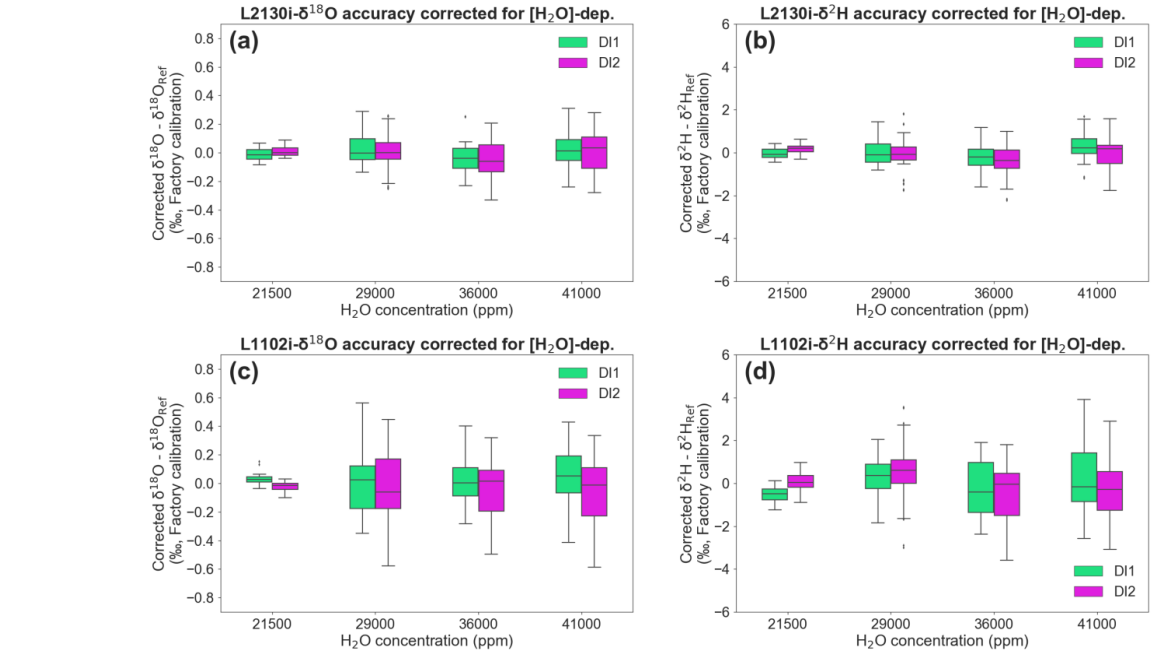

Figure 8 Deviations of $\delta^{18}O$ and $\delta^{2}H$, both corrected for [H_2O]-dependence, for each standard water (DI1 and DI2) at four different H_2O concentrations. Boxplots of (a) $\delta^{18}O$ and (b) $\delta^{2}H$ deviations, corrected for [H_2O]-dependence of L2130i. Boxplots of (c) $\delta^{18}O$ and (d) $\delta^{2}H$ deviations, corrected for [H_2O]-dependence of L1102i. The [H_2O]-dependence of each CRDS analysers was corrected by the DI1-2*2Pairs calibration strategy with the best fitting methods (L2130i and L1102i-$\delta^{2}H$: linear-surface fitting, L1102i-$\delta^{18}O$: cubic fitting) at 28 h interval.

4 Conclusions

This study extends previous work documenting water vapour concentration dependence of Picarro CRDS analysers to high moisture (> 35,000 ppm H_2O) likely to be measured in the Amazon rainforest. We assessed the precision and accuracy of two CRDS analysers (i.e., model L1102i and L2130i) for concentration and isotopic measurements by using a custom-made calibration unit that regularly supplied standard water vapour samples at four different H_2O concentrations between 21,500 and 41,000 ppm to the CRDS analysers. Our results demonstrate that the newer version of the analyser (L2130i) has better precision for both $\delta^{18}O$ and $\delta^{2}H$ measurements under all moisture conditions compared to the older model (L1102i). In addition, isotope measurements in both analysers varied with moisture content, especially at [H_2O]>36,000 ppm. The concentration dependence of the L1102i analyser was stronger than the L2130i analyser. These findings indicate that calibrating the [H_2O]-dependence of $\delta^{18}O$ and $\delta^{2}H$ measurements for both the CRDS analysers during field deployment in high atmospheric moisture areas such as tropical forests is important.

Assuming continuous in situ observation together with regular calibration in tropical Amazon rainforest, we devised four calibration strategies, adjusted to our custom-made calibration system, and then evaluated which [H_2O]-dependence calibration procedure best improved the accuracy of $\delta^{18}O$ and $\delta^{2}H$ measurements for both the L2130i and L1102i analysers. The best [H_2O]-dependence strategy was the DI1-2*2Pairs strategy that required two pairs of a two-point calibration with different moisture levels from 21,500 to 41,000 ppm. The 28 h interval strategy with the linear-surface fitting method leads to the most accurate measurements for both the CRDS analysers, except $\delta^{18}O$ accuracy of the L1102i analyser that required the cubic fitting method. In addition, [H_2O]-dependence calibration uncertainties hardly changed at any interval over 8 days. That indicates one [H_2O]-dependence calibration per week is sufficient for correcting moisture-biased isotopic accuracy of

https://doi.org/10.5194/amt-2020-305
Preprint. Discussion started: 2 September 2020

Atmospheric Measurement Techniques Discussions

the CRDS analysers. Nevertheless, to stay on the safe side, we decided to conduct the [H_2O]-dependence calibration at 28 h or less interval. The best calibration strategy at 28 h interval supported that both the CRDS analysers can sufficiently distinguish temporal variations of water vapour isotopes in the aimed ATTO site.

Data availability

All the data used in this publication are freely available at the "https://dx.doi.org/10.17617/3.4n."

Author contribution

The calibration system was designed and developed by SK, JL, TS and US. The laboratory experiments were conducted by SK with assistance from JL, TS, US and FK. The IRMS analysis was done by HM and HG. DW helped us to check water vapour concentration in the ATTO site. SK conducted the data-analysis and wrote the manuscript with assistance from JL, FK, and HM.

Competing interests

The authors declare that they have no conflict of interest.

Acknowledgements

This research was supported by German-Brazilian project ATTO, supported by the German Federal Ministry of Education and Research (BMBF contracts 01LB1001A and FKR 01LK1602A) and the Brazilian Ministério da Ciência, Tecnologia e Inovação (MCTI/FINEP contract 01.11.01248.00) as well as the Max-Planck Society. We are grateful to Susan Trumbore (MPI-BGC) for reviewing the earlier manuscript and her valuable feedback, to Stefan Wolff and Matthias Sörgel (MPI-Chemistry) for helping us to check H_2O concentration in the ATTO site, and also to Jürgen M. Richter (MPI-BGC) for helping us to prepare the DI1 and DI2 standard waters.

References

Aemisegger, F., Sturm, P., Graf, P., Sodemann, H., Pfahl, S., Knohl, A. and Wernli, H.: Measuring variations of $\delta^{18}O$ and $\delta^{2}H$ in atmospheric water vapour using two commercial laser-based spectrometers: An instrument characterisation study, Atmospheric Measurement Techniques, 5(7), 1491–1511, doi:10.5194/amt-5-1491-2012, 2012.

Andreae, M. O., Acevedo, O. C., Araùjo, A., Artaxo, P., Barbosa, C. G. G., Barbosa, H. M. J., Brito, J., Carbone, S., Chi, X., Cintra, B. B. L., da Silva, N. F., Dias, N. L., Dias-Júnior, C. Q., Ditas, F., Ditz, R., Godoi, A. F. L., Godoi, R. H. M., Heimann, M., Hoffmann, T., Kesselmeier, J., Könemann, T., Krüger, M. L., Lavric, J. V., Manzi, A. O., Lopes, A. P., Martins, D. L., Mikhailov, E. F., Moran-Zuloaga, D., Nelson, B. W., Nölscher, A. C., Santos Nogueira, D., Piedade, M. T. F., Pöhlker, C., Pöschl, U., Quesada, C. A., Rizzo, L. V., Ro, C.-U., Ruckteschler, N., Sá, L. D. A., de Oliveira Sá, M., Sales, C. B., dos Santos, R. M. N., Saturno, J., Schöngart, J., Sörgel, M., de Souza, C. M., de Souza, R. A. F., Su, H., Targhetta, N., Tóta, J., Trebs, I., Trumbore, S., van Eijck, A., Walter, D., Wang, Z., Weber, B., Williams, J., Winderlich, J., Wittmann, F., Wolff, S. and Yáñez-Serrano, A. M.: The Amazon Tall Tower Observatory (ATTO): overview of pilot measurements on ecosystem ecology, meteorology, trace gases, and aerosols, Atmos. Chem. Phys., 15(18), 10723–10776, doi:10.5194/acp-15-10723-2015, 2015.

https://doi.org/10.5194/amt-2020-305
Preprint. Discussion started: 2 September 2020

Bailey, A., Noone, D., Berkelhammer, M., Steen-Larsen, H. C. and Sato, P.: The stability and calibration of water vapor isotope ratio measurements during long-term deployments, Atmos. Meas. Tech., 8(10), 4521–4538, doi:10.5194/amt-8-4521-2015, 2015.

Coe, M. T., Macedo, M. N., Brando, P. M., Lefebvre, P., Panday, P. and Silvério, D.: The Hydrology and Energy Balance of the Amazon Basin, in Interactions Between Biosphere, Atmosphere and Human Land Use in the Amazon Basin, edited by L. Nagy, B. R. Forsberg, and P. Artaxo, pp. 35–53, Springer, Berlin, Heidelberg., 2016.

Delattre, H., Vallet-Coulomb, C. and Sonzogni, C.: Deuterium excess in the atmospheric water vapour of a Mediterranean coastal wetland: regional vs. local signatures, Atmos. Chem. Phys., 15(17), 10167–10181, doi:10.5194/acp-15-10167-2015, 2015.

Galewsky, J., Steen-Larsen, H. C., Field, R. D., Worden, J., Risi, C. and Schneider, M.: Stable isotopes in atmospheric water vapor and applications to the hydrologic cycle: ISOTOPES IN THE ATMOSPHERIC WATER CYCLE, Rev. Geophys., 54(4), 809–865, doi:10.1002/2015rg000512, 2016.

Gehre, M., Geilmann, H., Richter, J., Werner, R. A. and Brand, W. A.: Continuous flow $^{2}H/^{1}H$ and $^{18}O/^{16}O$ analysis of water samples with dual inlet precision, Rapid Communications in Mass Spectrometry, 18(22), 2650–2660, doi:10.1002/rcm.1672, 2004.

Helliker, B. R. and Noone, D.: Novel Approaches for Monitoring of Water Vapor Isotope Ratios: Plants, Lasers and Satellites, in Isoscapes: Understanding movement, pattern, and process on Earth through isotope mapping, edited by J. B. West, G. J. Bowen, T. E. Dawson, and K. P. Tu, pp. 71–88, Springer Netherlands, Dordrecht., 2010.

IAEA/WMO: https://nucleus.iaea.org/wiser, last access: 30 July 2020.

Intergovernmental Panel on Climate Change, Ed.: Detection and attribution of climate change: From global to regional, in Climate change 2013 - the physical science basis, pp. 867–952, Cambridge University Press, Cambridge., 2014.

Matsui, E., Salati, E., Ribeiro, M. N. G., Reis, C. M., Tancredi, A. C. S. N. F. and Gat, J. R.: Precipitation in the Central Amazon basin:-The isotopic composition of rain and atmospheric moisture at Belém and Manaus, Acta Amaz., 13(2), 307–369, doi:10.1590/1809-43921983132307, 1983.

Moreira, M., Sternberg, L., Martinelli, L., Victoria, R., Barbosa, E., Bonates, L. and Nepstad, D.: Contribution of transpiration to forest ambient vapour based on isotopic measurements. Global Change Biology, 3(5), 439-450, doi: 10.1046/j.1365-2486.1997.00082.x, 1997.

Schmidt, M., Maseyk, K., Bariac, T. and Seibt, U.: Concentration effects on laser-based $\delta^{18}O$ and $\delta^{2}H$ measurements and implications for the calibration of vapour measurements with liquid standards, Rapid Commun. Mass Spectrom., 9, doi:10.1002/rcm.4813, 2010.

Steen-Larsen, H. C., Sveinbjörnsdottir, A. E., Peters, A. J., Masson-Delmotte, V., Guishard, M. P., Hsiao, G., Jouzel, J., Noone, D., Warren, J. K. and White, J. W. C.: Climatic controls on water vapor deuterium excess in the marine boundary layer of the North Atlantic based on 500 days of in situ, continuous measurements, Atmos. Chem. Phys., 14(15), 7741–7756, doi:10.5194/acp-14-7741-2014, 2014.

Tremoy, G., Vimeux, F., Cattani, O., Mayaki, S., Souley, I. and Favreau, G.: Measurements of water vapor isotope ratios with wavelength-scanned cavity ring-down spectroscopy technology: New insights and important caveats for deuterium excess measurements in tropical areas in comparison with isotope-ratio mass spectrometry, Rapid Commun. Mass Spectrom., 25(23), 3469–3480, doi:10.1002/rcm.5252, 2011.

Wei, Z., Lee, X., Aemisegger, F., Benetti, M., Berkelhammer, M., Casado, M., Caylor, K., Christner, E., Dyroff, C., García, O., González, Y., Griffis, T., Kurita, N., Liang, J., Liang, M.-C., Lin, G., Noone, D., Gribanov, K., Munksgaard, N. C., Schneider, M., Ritter, F., Steen-Larsen, H. C., Vallet-Coulomb, C., Wen, X., Wright, J. S., Xiao, W. and Yoshimura, K.: A global database of water vapor isotopes measured with high temporal resolution infrared laser spectroscopy, Sci Data, 6(1), 180302, doi:10.1038/sdata.2018.302, 2019.